Eur Biophys J (2000) 29: 221–227

ARTICLE

David G. Regan · Philip W. Kuchel

Mean residence time of molecules diffusing in a cell bounded by a semi-permeable membrane: Monte Carlo simulations and an expression relating membrane transition probability to permeability

Received: 7 January 2000 / Revised version: 4 April 2000 / Accepted: 4 April 2000

Abstract The rapid exchange of water across erythrocyte membranes is readily measured using an NMR method that entails doping a suspension of cells with a moderately high concentration of Mn^{2+} and measuring the rate of transverse relaxation of the nuclear magnetisation. Analysis of the data yields an estimate of the rate constant for membrane transport, from which the membrane permeability can be determined. It is assumed in the analysis that the efflux rate of the water is solely a function of the rate of membrane permeation and that the time it takes for intracellular water molecules to diffuse to the membrane is relatively insignificant. The limits of this assumption were explored by using random-walk simulations of diffusion in cells modelled as parallel planes, spheres, and biconcave discs. The rate of membrane transport was specified in terms of a transition probability but it was not initially clear what the relationship should be between this parameter and the diffusional membrane permeability P_d. This relationship was derived and used to show that the mean residence time for a water molecule is determined by P_d when the diffusion coefficient is above a certain threshold value; it is determined by the distance to the membrane below that value.

Key words Membrane permeability · Parallel planes · Sphere · Biconcave disc · Bounded diffusion

Introduction

Molecular diffusion is a key process in facilitating chemical interactions in biological systems (e.g., Waldeck et al. 1997). The molecules in a cell are immersed in an aqueous medium and random motions that correspond to thermal energy fluctuations lead to molecular migration through the cell. This motion satisfies the proximity requirements for molecular interactions and may, in certain cases, constitute the rate-limiting step in these interactions.

In cellular systems, diffusion-mediated processes are constrained by three main parameters: (1) the intrinsic rate of diffusion (characterised by the diffusion coefficient D) in the intracellular medium; (2) the geometrical shape and dimensions of the cell; and (3) the rate of exchange of the molecular species across the cell membrane. Two of these parameters, diffusion coefficient and membrane exchange rate constant, are incorporated in a property of the cell membrane which is referred to as the permeability, that is denoted by P_d (Stein 1986). Thus, the permeability with respect to a particular molecule will be a function of both the rate of diffusion to the membrane and the rate of exchange across it.

The average length of time that a molecule spends inside a cell before exiting is referred to as the mean residence time (MRT); it is a function of the permeability of the cell membrane with respect to that molecule, and the geometrical form and dimensions of the cell. If the mean time taken for a class of molecule to diffuse across the interior of a cell is comparable to the experimentally measured MRT, then it can be inferred that the membrane does little to impede the efflux from the cell. On the other hand, if the MRT is much greater than this diffusion time, then the inference can be made that the permeability of the membrane is what controls the efflux.

The challenges of the work described here were threefold: (1) to develop a model of molecular diffusion in cells in order to simulate experimental data used in estimating the MRT of water in red blood cells (RBC); (2) to derive a mathematical expression relating membrane transition probability (see Methods) and P_d; and (3) to use the data from the simulations, in conjunction with the permeability expression, to calculate the parameter ranges, for various geometries (parallel planes,

D.G. Regan · P.W. Kuchel (✉)
Department of Biochemistry, University of Sydney,
NSW 2006, Australia
e-mail: p.kuchel@biochem.usyd.edu.au

spheres, and biconcave discs), that determine whether the MRT is dominated by membrane permeability or the cell dimensions. The motivation for the second of these goals arose from the initial finding that MRT, as predicted by computer simulations of membrane-bounded diffusion, depended on the jump length (see Methods) chosen in the simulations.

The computer simulations employed a random walk technique, based on a Monte Carlo method, to simulate the diffusion of water inside a virtual cell that could be described by a mathematical expression in three Cartesian dimensions (e.g., Lennon and Kuchel 1994a, b; Lennon et al. 1994). The predicted MRT values were compared with those calculated from NMR relaxation data obtained using the so-called manganese-doping method (Benga et al. 1990, 1992, 1993).

Theory

Random walk simulations of diffusion

The Monte Carlo random walk procedures used in this work have been described previously (Lennon and Kuchel 1994a, b; Lennon et al. 1994) and specific details of their implementation are given in Methods. However, a general overview of the method is warranted in order to provide a context for the derivation of a mathematical expression for P_d.

Random walks can be implemented in any number of dimensions. In a three-dimensional random walk, a cubic lattice provides a convenient representation of the medium through which a virtual particle (or an ensemble of independent particles) diffuses by jumping from lattice point to lattice point. The distance between adjacent lattice points is the jump length (s) and the time taken to undergo a single jump is the jump time. A single three-dimensional jump is achieved by simultaneously updating the coordinates of the particle by + or – one jump length in the x, y, and z directions (assuming the lattice is aligned with the x-, y-, and z-Cartesian axes). The direction of displacement (+ or –) in each dimension is chosen at random, by means of a random number generator (RNG; specifically, a random binary digit generator). The choice of s and jump time are related to the diffusion coefficient assigned to the virtual particle. The average coordinate after time t for an ensemble of point molecules, starting at the origin and diffusing freely and isotropically, will be zero. However, the mean square displacement, $\langle r^2 \rangle$, for the ensemble in three dimensions is given by the Einstein equation:

$$\langle r^2 \rangle = 6Dt \tag{1}$$

In a system where diffusion is restricted by barriers (bounded diffusion), that may be impermeable or semi-permeable, the apparent (experimentally observed) diffusion coefficient (D_{app}) will be smaller than the intrinsic diffusion coefficient, i.e., the mean-square displacement in a given time will be smaller than for free diffusion. By considering Eq. (1) it is seen that this effect becomes pronounced when the time interval during which diffusion is observed, τ, is large in comparison with the ratio a^2/D, where a is the separation distance between the barriers. Hence, in the case of a sphere, bounded diffusion will be observed when $\tau \gg \sim a^2/D$, where a is the radius of the sphere.

When diffusion is restricted by a semi-permeable membrane, the simulation of this property is achieved by defining the spatial location of the barrier (namely, $x^2 + y^2 + z^2 = a^2$ for a sphere) and ascribing to it a transition probability (tp) which determines the probability of transition by a virtual particle upon intersection of its trajectory with the barrier. The diffusive permeability coefficient, P_d, for a slice of a membrane of unit area is given by (Stein 1986):

$$P_d = D/\lambda \tag{2}$$

where D is the diffusion coefficient of the diffusant in the membrane and λ is the thickness of the membrane (see Fig. 1). The permeability coefficient has the dimensions m s^{-1}, which is consistent with the notion that it is a measure of the rate at which a substance crosses the membrane, and it corresponds to the reciprocal of the diffusive resistance. Fick's first law of diffusion specifies that the flux, J_d, through unit area of membrane orthogonal to the flux is equal to the diffusion coefficient of the diffusant multiplied by its concentration gradient in the direction of the flux:

$$J_d = -D(C_2 - C_1)/\lambda = -P_d(C_2 - C_1) \tag{3}$$

Because we do not usually know the effective thickness or how the concentration gradient varies within a biological membrane, the permeability is usually used as an experimentally more convenient measure of flux through the membrane than the diffusion coefficient (Stein 1986).

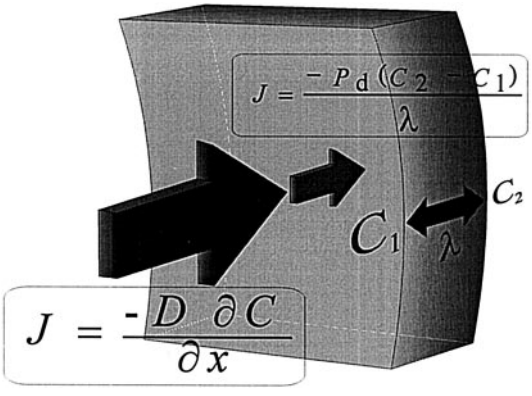

Fig. 1 Schematic representation of flux (J, *large single-headed arrow*) to the membrane and through the membrane (J, *small single-headed arrow*). The concentration difference across the membrane is equal to $C_2 - C_1$, and the membrane thickness is denoted by λ which corresponds to jump length (s) in the context of the Monte Carlo random walk

Relationship between tp and P_d

The transition probability of a membrane is the rate of transfer across the membrane, J_{mem} (represented by the small arrow in Fig. 1), relative to that which would occur in the same region of space in the absence of the membrane, J_{bulk} (the large arrow in Fig. 1); thus:

$$tp = \frac{J_{mem}}{J_{bulk}} = \frac{P_d(C_2 - C_1)}{D\partial C/\partial x} \quad (4)$$

An individual particle jumps, at each step of its random walk, from its current position at concentration C_1 to its new position at concentration C_2. Because each trajectory is independent of all others, each step is, in effect, a step into an unoccupied volume whose concentration (C_2) is therefore zero; this is true both for diffusion in the bulk medium and for transition across the membrane. While concentration has little physical meaning for a single particle, it is heuristically useful to consider the concentration at C_1 and C_2 as being separated by the distance s, equal to the jump length, and so the partial derivative in the denominator of Eq. (4) can be written as $(C_2 - C_1)/s = -C_1/s$. Equation (4) then simplifies to:

$$tp = \frac{P_d s}{D} \quad (5)$$

or

$$P_d = \frac{D\,tp}{s} \quad (6)$$

Thus, s, in effect, represents the membrane thickness as a result of the particular way the membrane boundary is defined. In words, Eq. (6) indicates that a reduction in the transition probability will result in a smaller value for P_d, while a reduction in the thickness of the membrane will result in a larger value. Thus, in a Monte Carlo simulation, the permeability can be kept constant by ensuring that the ratio tp/s is held constant.

Methods

Monte Carlo simulations

The basic procedures and programs employed in simulating bounded molecular diffusion have been described previously (Lennon and Kuchel 1994a, b; Lennon et al. 1994). The original programs, written in C, were modified to allow the calculation of MRT values under prescribed conditions, while various redundancies were eliminated to enable increased computational speed.

Simulations were performed for ensembles of non-interacting point molecules having an intrinsic diffusion coefficient of $D = 2.0 \times 10^{-9}$ m^2 s^{-1}, which is approximately equal to that of water at 20 °C (Mills 1973).

Diffusion was restricted to the region of space enclosed either by parallel planes, a sphere, or a biconcave disc (Fig. 2). These boundaries were specified as being semi-permeable by assigning them a value of tp, which was invoked upon intersection of a trajectory of a point molecule with the boundary.

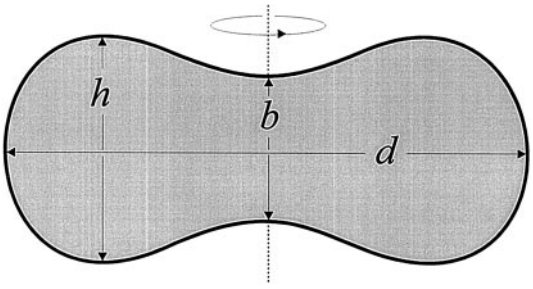

Fig. 2 Two-dimensional representation of a biconcave disc whose shape and dimensions are defined by means of the parameters b, d, and h. Rotation around the axis indicated by the *dotted line* results in a three-dimensional model which approximates the shape of a human red blood cell

The biconcave disc (or discocyte) was represented by a degree-4 equation in Cartesian coordinates (Kuchel and Fackerell 1999). This defines a shape by means of three parameters (see Fig. 2) that closely approximates the shape of a human red blood cell ($b = 1.0 \times 10^{-6}$ m, $h = 2.12 \times 10^{-6}$ m, $d = 8.0 \times 10^{-6}$ m) or of an elephant red blood cell ($b = 1.16 \times 10^{-6}$ m, $h = 2.3 \times 10^{-6}$ m, $d = 9.3 \times 10^{-6}$ m) (Benga et al. 1999).

For diffusion within spherical boundaries, a radius of 5.0×10^{-6} m was chosen. For diffusion bounded by parallel planes, the distance separating the planes was either 1.5×10^{-6} m (a distance which represented approximately the average distance between the flattish surfaces of a human RBC) or 5.0×10^{-6} m.

The diffusion coefficient, tp, and s could also be independently varied, allowing membrane permeability to be manipulated in a number of ways. Comparison of simulation data with analytical results for diffusion between perfectly reflecting parallel planes (Piton et al. 1994) implied that the ratio of the dimension separating the planes to jump length should be at least 5:1 for consistent results and this principle was applied in all simulations.

Calculation of MRT

In order to calculate the MRT for an ensemble of point molecules diffusing in a system bounded by semi-permeable boundaries, each point molecule began its trajectory from a randomly chosen location inside the bounded compartment and was allowed to continue its trajectory until it crossed the membrane. The times spent inside the compartment, prior to membrane transition, were summed and averaged over the entire ensemble consisting of 1000 individual point molecules, to yield an MRT for the particular parameter set.

Results

The original aim of the work was to use Monte Carlo simulations to corroborate MRT data that had been acquired from human RBC, and for other species, using the NMR manganese-doping procedure (Benga et al. 1990, 1992, 1993). Thus, it was necessary to establish the nature of the relationship between *tp* and P_d, the latter of which can be measured experimentally for real cells. The preliminary simulations revealed an interesting phenomenon: while the predicted MRT was a function of *tp* as expected (a smaller value of *tp* resulted in a larger MRT), it was observed that if the jump length was decreased the MRT also decreased. In other words, the MRT appeared to be also dependent on *s*. This outcome was initially felt to be counterintuitive but the derivation of Eq. (6) revealed the logic of the phenomenon.

Figure 3 shows the results of simulations in which the MRT values were calculated for parallel planes (separation distance, 5×10^{-6} m), a sphere (radius, 5×10^{-6} m), and a biconcave disc (having the dimensions of human RBC; see Methods), with three different values of *tp*: 0.1, 0.01, and 0.001. The range of jump lengths varied from $s_{min} = 1/5 \times a$ to $s_{max} = 1/10{,}000 \times a$ ($s_{max} = 1/20{,}000 \times a$ in the case of parallel planes), where *a* was equal to the distance separating the parallel planes, the radius of the sphere, or the dimension *b* in the biconcave disc (Kuchel and Fackerell 1999; see Fig. 2). Figure 3 shows that the MRT values increased as *tp* was reduced at any value of *s*. This was expected since a reduction in *tp* reduces the number of collisions with the membrane, which on average are required for exit from the cell. However, MRT values also decreased as *s* was reduced for a given value of *tp*. Figure 3 also shows that MRT values converged asymptotically to a limiting value as *s* became small.

Table 1 contains the data used to generate Fig. 3A (parallel planes) and it illustrates the important finding that any two simulations in which *tp* differed by a factor of, say, 10 yielded approximately the same value of MRT as when *s* differed by the same proportion for a given *tp*. Specifically, the MRT equalled 1.154 ms when *tp* was 0.1 and *s* was 1×10^{-8} m, and it also equalled 1.156 ms when *tp* was 0.01 and *s* was 1×10^{-9} m. Similar results were observed for the sphere and the biconcave disc (data not shown).

Figure 4 shows the relationship between MRT and *D*, when P_d is held constant. For this series of simulations, *D* was increased by a factor of two in 11 steps from a minimum of 1.5625×10^{-11} m^2 s^{-1} to a maximum of 1.6×10^{-8} m^2 s^{-1}. P_d was maintained at a constant, predetermined, value by adjusting the value of *tp* using Eq. (6). Four sets of simulations were conducted using the following boundaries: parallel planes, 1.5×10^{-6} m separation; sphere, 5×10^{-6} m radius; biconcave disc, human RBC dimensions; biconcave disc, elephant RBC dimensions. A P_d of 6.1×10^{-5} m s^{-1} was used for the parallel planes, sphere, and human RBC as this value had been determined experimentally for human RBC (Benga et al. 1990). For the elephant RBC, P_d was set to 5.2×10^{-5} m s^{-1}, as was recently determined experimentally (Benga et al. 1999). For Fig. 4A, the MRT values simulated for human RBC were plotted as a function of *D* (main graph) and as a function of D^{-1} (inset); these transformed data were well represented by a straight line and for purposes of illustration they were fitted using Microcal Origin (Microcal Software, Northampton, Mass., USA). The fitting yielded $MRT_{human\ RBC} = 2.08 \times 10^{-10}/D + 11.87$ ms. On the other hand, the untransformed data clearly revealed that below a particular value of *D* the MRT increases

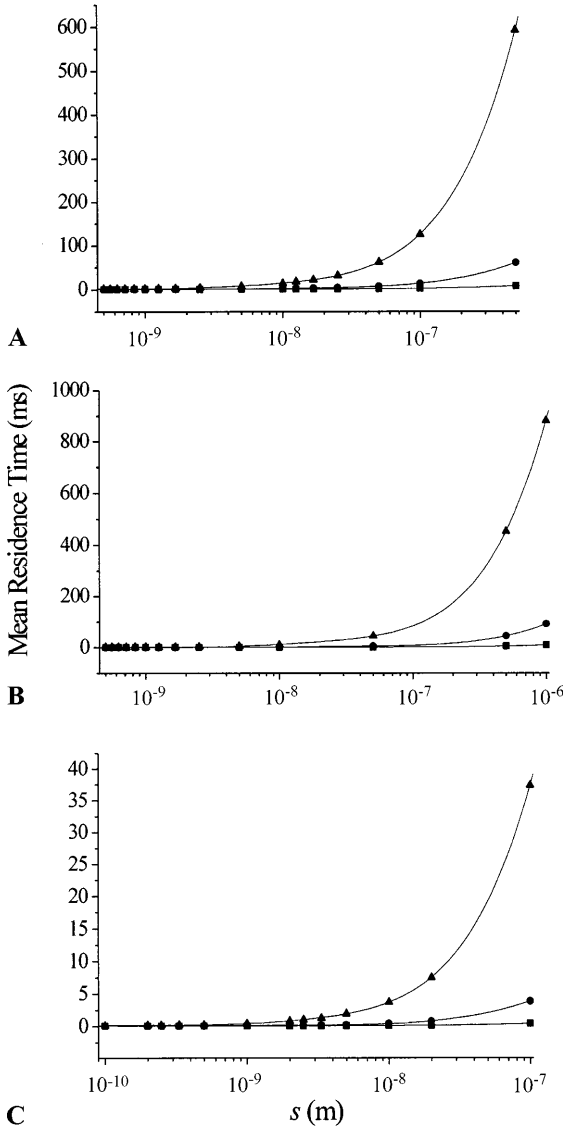

Fig. 3 MRT as a function of jump length (*s*) for parallel planes (**A**), sphere (**B**), and biconcave disc (**C**) for *tp* = 0.1 (■), *tp* = 0.01 (●), and *tp* = 0.001 (▲). The parallel planes were separated by a distance of 5×10^{-6} m. The radius of the sphere was 5×10^{-6} m. The biconcave disc had the dimensions $b = 1.0 \times 10^{-6}$ m, $d = 8.0 \times 10^{-6}$ m, and $h = 2.12 \times 10^{-6}$ m (see Fig. 2) so as to approximate the size and shape of the human RBC

Table 1 Mean residence times (MRT) for parallel planes at three values of transition probability and as a function of jump length. The planes were separated by a distance of 5×10^{-6} m. MRT values for individual simulations were calculated by averaging over an ensemble of 1000 independent trajectories of point molecule

s ($10^6 \times$ m)	MRT (ms)		
	$tp = 0.1$	$tp = 0.01$	$tp = 0.001$
0.5	7.363	60.161	591.031
0.1	2.260	13.380	124.461
0.05	1.680	6.987	61.709
0.025	1.317	4.093	31.350
0.0167	1.225	3.184	21.716
0.0125	1.086	2.474	17.800
0.01	1.154	2.391	13.561
0.005	1.078	1.615	7.516
0.0025	1.015	1.293	4.167
0.00167	1.109	1.275	2.978
0.00125	1.012	1.213	2.616
0.001	1.008	1.156	2.491
0.000833	1.071	1.063	2.187
0.000714	1.051	1.069	1.984
0.000625	1.039	1.210	1.876
0.000556	1.012	1.196	1.850
0.0005	1.107	1.171	1.705
0.00025	1.216	1.289	1.558

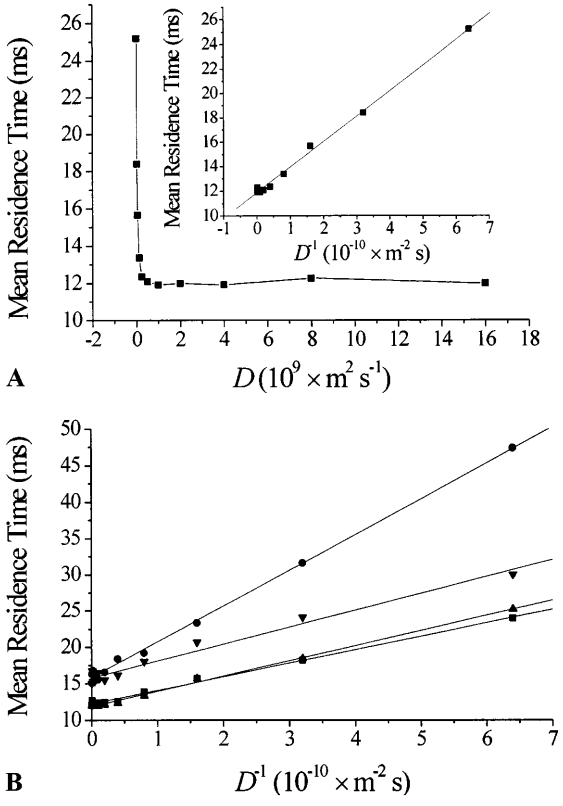

Fig. 4A, B MRT as a function of diffusion coefficient (D) at constant permeability. **A** shows the native data for a biconcave disc (human RBC dimensions, main axes) as well as a plot of MRT as a function D^{-1} to which a straight line was fitted (see Methods). **B** shows the linearised data for the sphere (●; radius $= 5 \times 10^{-6}$ m), elephant RBC (▼; $b = 1.16 \times 10^{-6}$ m, $d = 9.3 \times 10^{-6}$ m, $h = 2.3 \times 10^{-6}$ m), human RBC (▲; $b = 1.0 \times 10^{-6}$ m, $d = 8 \times 10^{-6}$ m, $h = 2.12 \times 10^{-6}$ m), and parallel planes (■; separation $= 1.5 \times 10^{-6}$ m)

sharply, whereas above that point (or local domain of values) their values remain almost constant. Figure 4B shows the linearised data from all four sets of simulations yielding the following fits: $\mathrm{MRT}_{\mathrm{sphere}} = 4.92 \times 10^{-10}/D + 15.81$ ms; $\mathrm{MRT}_{\mathrm{elephant\ RBC}} = 2.33 \times 10^{-10}/D + 15.76$ ms; $\mathrm{MRT}_{\mathrm{parallel\ planes}} = 1.85 \times 10^{-10}/D + 12.24$ ms. These results and their associated errors are summarised in Table 2.

The final two columns of Table 2 give the approximate values of D at which the MRT rises exponentially (D_{rise}), and the average value of MRT prior to that rise ($\mathrm{MRT}_{\mathrm{const}}$), namely the value of MRT in the region in which it is relatively constant. It should be noted that a difference of a factor of two exists for D between adjacent data points; it will be necessary to subject this region to scrutiny at higher resolution to determine the point of inflexion more accurately. Two additional points warrant noting:

(1) The linear correlation coefficient (r) in each case suggests a strong linear dependency of the transformed data. This is somewhat deceptive, however, since the data points for small values of D^{-1} are densely crowded near the origin and when this portion of the graph is expanded (not shown) the graph appears to be biphasic.

(2) The values in the last column ($\mathrm{MRT}_{\mathrm{const}}$) closely correspond to the constant term in the linear equation given in the second column (MRT).

The experimentally determined P_{d} for human and elephant RBC (Benga et al. 1990, 1999) were calculated

Table 2 Mean residence times for human RBC, elephant RBC, sphere, and parallel planes as a function of D when permeability was kept constant by adjusting tp. The second column (MRT) defines this relationship as approximately linear, as suggested by performing a linear regression on MRT versus D^{-1} data. The third column (SD) is the standard deviation, which provides an indication of the degree to which the actual data deviated from linear, as does the linear correlation coefficient (r) in the fourth column. D_{rise} is the diffusion coefficient below which the MRT began to rise rapidly, and $\mathrm{MRT}_{\mathrm{const}}$ is the average value of MRT for values of D above that value

	MRT (ms)	SD	r	D_{rise} ($\mathrm{m^2\ s^{-1}}$)	$\mathrm{MRT}_{\mathrm{const}}$ (ms)
$\mathrm{RBC}_{\mathrm{human}}$	$2.08 \times 10^{-10}/D + 11.87$	0.26	0.998	1.25×10^{-10}	12.08
$\mathrm{RBC}_{\mathrm{elephant}}$	$2.33 \times 10^{-10}/D + 15.76$	0.81	0.987	1.25×10^{-10}	15.8
Sphere	$4.92 \times 10^{-10}/D + 15.81$	0.58	0.998	5×10^{-10}	16.15
Parallel planes	$1.85 \times 10^{-10}/D + 12.24$	0.29	0.997	1.25×10^{-10}	12.36

from MRT values according to the following formula that interrelates cell volume (V), cell surface area (A), and MRT:

$$P_d = (V/A)(1/MRT) \quad (7)$$

In these calculations, a factor of 0.7 was applied to the V/A ratio to account for the fact that, in real cells, water only occupies ~70% of the total cell volume. Consequently, if the correction factor is eliminated, Eq. (6) predicts MRT for real and elephant RBC of 10.98 ms and 14.23 ms, respectively.

Discussion

Predictions of MRT values made from Monte Carlo random walk simulations of diffusion were compared with previously published results acquired experimentally from RBC. In exploring the validity of the analysis, three model systems were chosen, namely parallel planes, spheres, and biconcave discs. In order for the simulated RBC system to closely correspond to the real one, it was necessary to define the relationship between transition probability (tp) and permeability (P_d).

It initially seemed counter intuitive that a variation in jump length (s) [with its corresponding variation in jump time, via Eq. (1)] should lead to a variation in MRT (Fig. 3). However, once Eq. (6) had been derived, the basis of this phenomenon became apparent. Because a decrease in jump length (s) effectively specifies a decrease in membrane thickness (λ), the result is an increase in P_d [via Eq. (2)]. Conversely, Eq. (6) implies that a decrease in D and/or tp will result in a reduction of P_d. Both of these assertions are consistent with the idea that a reduction in D will increase the time taken for the diffusing molecule to reach the membrane, while a reduction in tp reduces the likelihood of exit once the membrane is reached.

Figure 3 also illustrates that as s becomes very small, such that P_d is high, there is little change in the value of MRT; this is consistent with Eq. (6). Figure 1 also shows that for a biconcave disc whose disc planes are separated by 1–2 μm, the MRT at a particular value of s and tp is much smaller than for parallel planes separated by 5 μm or spheres of radius 5 μm at the same values of s and tp. This observation points to the fact that MRT is not only a function of P_d but also of the geometry and dimensions of the confining region.

From Table 1 it can be seen that for any two simulations at constant D, when the ratios tp/s are equal, the values of MRT obtained are also approximately equal. This underscores the numerical interaction between the parameters that determine the value of P_d, via Eq. (6).

When P_d is constant, MRT remains almost constant for values of D above a certain value (Fig. 4). When D is less than that value, the MRT increases sharply, indicating that the dominant factor in determining MRT is now the time required to diffuse through the average distance to the membrane from a randomly chosen starting point inside the cell, and not the permeability of the membrane. The inset in Fig. 4A reveals a second finding: an approximately linear relationship exists between MRT and the reciprocal of D and this conformity is better at higher values of D^{-1}. Table 2 also shows that the intercept of the fitted line with the ordinate (i.e., when $D \to \infty$) corresponds to a value of MRT that is approximately equal to the average MRT_{const} value. The threshold occurs at $D \approx 1.25 \times 10^{-10}$ in all cases except for the sphere ($D \approx 5 \times 10^{-10}$), reflecting the fact that for parallel planes, RBC_{human}, and $RBC_{elephant}$ the dimensions are such that the distances between boundaries were in the region of 1–2 μm; for the sphere ($r = 5$ μm) the average distance between boundaries was greater and therefore the threshold below which this factor was the dominant one in determining MRT was higher.

The data in Fig. 4B further illustrate the difference between the sphere and the other shapes with respect to the dependence of MRT on the parameters chosen for the simulations. The values of MRT calculated from parallel planes separated by 1.5 μm closely approximated those for human RBC. The elephant RBC has a greater volume (Benga et al. 1999), so the slightly higher MRT is attributed to a greater separation between the disc planes of the cell. The MRT values of 10.98 ms and 14.23 ms obtained experimentally for real human and elephant RBC, respectively, are in close agreement with those obtained in the Monte Carlo simulations (~12 ms and ~16 ms for human and elephant RBC, respectively, see Table 2).

Finally, it is acknowledged that the models of restricted diffusion used in the simulations involved several fundamental assumptions.

(1) The equation used to describe the RBC is only an approximation of the actual shape (Kuchel and Fackerell 1999); previous work has shown, however, that small departures from real relative dimensions have little effect on the estimated MRT (unpublished data).
(2) Point molecules were assumed to diffuse independently and unimpeded in the entire volume of the cell, whereas in real cells water occupies only ~70% of the cell volume.
(3) For the sake of consistency, the diffusion coefficient was set to 2.0×10^{-9} m^2 s^{-1} for all models; this value is higher than that determined experimentally for diffusion of water inside RBC ($\sim 8.0 \times 10^{-10}$ for human RBC, unpublished data); however, both these values lie well within the region in which MRT is relatively constant (Fig. 4).
(4) The sub-membrane cytoskeleton, the finite thickness of the membrane, and other structural features of cells were absent from the RBC model; these could be incorporated in a more comprehensive model.

Thus, while the model could be refined, even in its present form it illustrates several key factors that influence the MRT of molecules in cells. It also introduces a means of studying the factors that limit the applicability of the data analysis used in the manganese-doping experiments (e.g., Benga et al. 1990).

Conclusions

An expression that relates tp and s to P_d in a Monte Carlo random walk simulation of diffusion and membrane transport in cells was derived (Eq. 6). The veracity of the equation was established using simulations (Table 1). When the mean distance traversed in the experimentally determined MRT is long relative to the cell dimensions, then it is the value of P_d that will determine the MRT. A quantitative understanding of this result has important implications for the constraints on cell size and MRT that are important in the kinetics of cellular events.

Monte Carlo simulations of diffusion are a potentially useful and sensitive method for determining the MRT for molecular species in cellular and other bounded systems. Future work could include more elaborate models of the cell boundaries that better reflect the complexity of real systems than those used herein.

Acknowledgements The work was supported by a grant from the Australian Research Council. D.G.R. acknowledges the award of a Commonwealth of Australia Postgraduate Scholarship. Professor Gheorghe Benga is thanked for valuable discussions on the manganese-doping method, and Bill Lowe is thanked for expert technical assistance.

References

Benga G, Pop VI, Popescu O, Borza V (1990) On measuring the diffusional water permeability of human red blood cells and ghosts by nuclear magnetic resonance. J Biochem Biophys Methods 21: 87–102

Benga Gh, Popescu O, Pop VI, Hodor P, Borza T (1992) Effects on water diffusion of inhibitors affecting various transport processes in human red blood cells. Eur J Cell Biol 59: 219–223

Benga Gh, Chapman BE, Gallagher CH, Agar NS, Kuchel PW (1993) NMR studies of diffusional water permeability of erythrocytes from eight species of marsupial. Comp Biochem Physiol 106A: 515–518

Benga Gh, Kuchel PW, Chapman BE, Cox GC, Ghiran I, Gallagher CH (1999) Comparative cell shape and diffusional water permeability of red blood cells from Indian elephant (*Elephas maximus*) and man (*Homo sapiens*). Comp Haemotol Int (in press)

Kuchel PW, Fackerell ED (1999) Parametric-equation representation of biconcave erythrocytes. Bull Math Biol 61: 209–220

Lennon AJ, Kuchel PW (1994a) Neural networks used to interpret pulsed-gradient restricted diffusion data. J Magn Reson A 107: 229–235

Lennon AJ, Kuchel PW (1994b) Enhancement of the ''diffraction-like'' effect in NMR diffusion experiments. J Magn Reson A 111: 208–211

Lennon AJ, Scott NR, Chapman BE, Kuchel PW (1994) Hemoglobin affinity for 2,3-bisphosphoglycerate in solutions and intact erythrocytes: studies using pulsed field gradient NMR and Monte Carlo simulations. Biophys J 67: 2096–2109

Mills R (1973) Self-diffusion in normal and heavy water in the range 1–45°. J Phys Chem 77: 685–688

Piton MC, Lennon AJ, Chapman BE, Kuchel PW (1994) Diffusion of solvent in swollen latex particles. J Colloid Interface Sci 166: 437–443

Stein WD (1986) Physical basis of movement across cell membranes. In: Stein WD, Lieb WR (eds) Transport and diffusion across cell membranes. Academic Press, Orlando, pp 173–181

Waldeck AR, Kuchel PW, Lennon AJ, Chapman BE (1997) NMR diffusion measurements to characterise membrane transport and solute binding. Prog NMR Spectrosc 30: 39–68